



Contents lists available at ScienceDirect

# Tunnelling and Underground Space Technology

journal homepage: [www.elsevier.com/locate/tust](http://www.elsevier.com/locate/tust)

## The effect of erosion voids on existing tunnel linings

M.A. Meguid\*, H.K. Dang

Department of Civil Engineering and Applied Mechanics, McGill University, 817 Sherbrooke Street West, Montreal, Quebec, Canada H3A 2K6

### ARTICLE INFO

#### Article history:

Received 10 February 2008  
 Received in revised form 10 September 2008  
 Accepted 13 September 2008  
 Available online 26 October 2008

#### Keywords:

Tunnel lining  
 Numerical simulation  
 Erosion voids  
 Lining stresses  
 Flexibility ratio

### ABSTRACT

Erosion voids may develop around buried infrastructures due to several reasons including water infiltration into leaking joints, dissolution of Karst limestone, and dynamic loading caused by construction related activities. This study evaluates the effect of erosion voids developing in the close vicinity of existing tunnels on the circumferential stresses in the lining. A series of simplified void geometries are defined beside and under the lining. Elasto-plastic finite element analyses are performed to study how those voids influence thrust forces and bending moments in the lining. The role of other factors such as the lining flexibility and in situ stress conditions is also investigated. Depending on the flexibility ratio between the lining and the surrounding soil, the void size can have a significant impact on the circumferential stresses in the tunnel lining. A void under the invert leads to decrease in the magnitude of bending moment, and for large void size, the moments can reverse sign. This preliminary study suggests that efforts to arrest the growth of erosion voids at the invert and springline should be made before the voids reach this size. All results presented are theoretical in nature, and physical testing is needed to evaluate the performance of these calculations.

© 2008 Elsevier Ltd. All rights reserved.

### 1. Introduction

Tunnels are considered to be one of the main underground structures and are widely used for transportation, waste water, electricity or communication cables, etc. With the new developments and upgrade of existing infrastructure, tunnel construction is increasing all over the world and tunnel engineers are more aware of the importance of the safety and economics of a tunnel design and construction. Peck (1969) stated three main issues to be considered in a successful tunnel design – first, maintaining stability and safety during construction, second, minimizing unfavourable impact on third party structures, and finally performing the intended function over the service life of a project.

In engineering practice different methods are often used to calculate lining stresses, including empirical (e.g. Peck, 1969; Schmidt, 1974; Attwell, 1978; O'Reilly and New, 1982; Mair et al., 1993); analytical (e.g. Schulze and Duddeck, 1964; Morgan, 1971; Peck et al., 1972; Muir Wood, 1975; Einstein and Schwartz, 1979; Sagaseta, 1987; Verruijt and Booker, 1996; Loganathan and Poulos, 1998; Bobet, 2001) and numerical analyses (e.g. Mair et al., 1981; Swoboda et al., 1989; Lee and Rowe, 1990; Leca and Clough, 1992; Chen and Baldauf, 1994; Augarde and Burd, 2001). These studies significantly contributed to the understanding of

the soil-lining interaction mechanisms under perfect contact conditions between the lining and the surrounding ground.

It has been observed that during the service life of a tunnel, the surrounding soils may erode locally around the lining as illustrated in Fig. 1. This condition may develop due to several reasons including water infiltration into leaky joints or a deteriorated lining system, dissolution of soils or nearby bedrock strata, and dynamic loading. Water ingress into tunnels may be encountered as well in the construction phase of any tunnel as in the operation phase of drained tunnels (Kolymbas and Wagner, 2007). The negative consequences of this process can vary from minor surface corrosion of tunnel appurtenances to major deterioration of the structure and thus decreased load carrying capacity of the tunnel. Most tunnels have problems that fall somewhere in between (U.S. Department of Transportation, 2005). Possible forms of degradation that can result from water infiltration into tunnels include: erosion of cement and sometimes aggregates of concrete liners causing the structure to be weakened; bolts that connect segmental linings can corrode and fail; fine soil particles can be carried through cracks with the water creating voids behind the liner, which can cause settlement of surrounding structures and/or cause eccentric loading on tunnel that can lead to unforeseen stresses.

Talesnick and Baker (1999) reported the failure of a large diameter (1.2 m) concrete-lined steel sewage pipe buried in clayey soils. Field investigations revealed the formation of a physical gap of approximately 20 mm between the invert and the bedding layer supporting the pipe. Severe cracking developed at the crown and springline along a 300 m segment of the pipeline. Although the

\* Corresponding author. Tel.: +1 514 398 1537; fax: + 1514 398 7361.

E-mail addresses: [mohamed.meguid@mcgill.ca](mailto:mohamed.meguid@mcgill.ca) (M.A. Meguid), [kien.dang@mail.mcgill.ca](mailto:kien.dang@mail.mcgill.ca) (H.K. Dang).

**Nomenclature**

$A_s, I_s$	area and moment of inertia of cross section of liner	$K_0$	coefficient of earth pressure at rest
$C, F$	compressibility and flexibility ratios	$L_v$	void length along the tunnel circumference
$E, \nu$	Young's modulus and Poisson's ratio of the soil	$p_{ref}$	reference pressure
$E_l, \nu_l$	Young's modulus and Poisson's ratio of the liner	$r$	tunnel radius
$E_{oed}, E_{50}, E_{ur}$	initial, secant and unloading moduli of the soil	$T, M$	axial force and moment acting on cross section of liner
$f_s$	the ratio between the stress at which the unloading starts and the stress at failure	$t, w$	lining thickness and gap between ground and liner
$k$	dimensionless modulus number	$c', \phi', \gamma$	cohesion, friction angle and unit wavelength of the soil
		$\sigma_1, \sigma_2$	major and minor principal stresses

pipe was installed using the conventional trench excavation method, this case study emphasizes the importance of a full contact between the buried structure and the supporting soil.

The objective of this study is to investigate the impact of erosion voids developed around existing tunnels on the circumferential stresses in the linings. A series of simplified void geometries are defined beside and under the lining. Elasto-plastic finite element analyses are performed to study how those voids influence thrust forces and bending moments in the lining. The role of other factors such as the lining flexibility and in situ stress condition is also investigated.

**2. Initial lining stresses**

Structural design models including analytical closed form solutions and bedded beam approaches have been extensively used by engineers for the analysis of both conventional and shield tunnelling. Installation procedures of these tunnelling methods (e.g. shield tunnelling, sequential excavation, etc.) significantly influence the magnitude and distribution of loads on tunnel lining and it has been discussed thoroughly in the literature. Schmid (1926) was probably the first to present an analytical solution for a continuum tunnel model. Later analytical solutions for bending moments and normal forces were presented by Bull (1944), Engelbreth (1961), Schulze and Duddeck (1964), Morgan (1971), Peck et al. (1972), Muir Wood (1975), Einstein and Schwartz (1979), Sagaseta (1987), Verruijt and Booker (1996), Loganathan and Poulos (1998), Bobet (2001), Chou and Bobet (2002).

In the above context, Peck et al. (1972) introduced the definition of stiffness ratios, which are the flexibility ratio and the compressibility ratio, for tunnel liners. The flexibility ratio ( $F$ ) is the flexural stiffness ratio between the ground and the liner and is defined as follows:

$$F = \frac{E}{(1 + \nu)} \bigg/ \frac{6E_l I_l}{r^3(1 - \nu_l^2)} \tag{1}$$

where  $E$  is the elastic modulus of the soil,  $E_l$  is the elastic modulus of the liner,  $I_l$  is the moment of inertia of the liner cross section per unit length along the tunnel axis, and  $r$  is the radius of the liner. The compressibility ratio ( $C$ ) is obtained by dividing the extensional stiffness of ground by that of the liner and is defined as follows:

$$C = \frac{E}{(1 + \nu)(1 - 2\nu)} \bigg/ \frac{E_l t}{r(1 - \nu_l^2)} \tag{2}$$

where  $t$  is the lining thickness,  $\nu$  is the Poisson's ratio of the soil, and  $\nu_l$  is the Poisson's ratio of the lining. For a given in situ stress condition (shown in Fig. 2), the moment,  $M$ , and thrust,  $T$ , in the liner can be theoretically obtained as follows:

$$M = \frac{Pr^2}{2} \left\{ (1 + K_0) \left[ \frac{(1 - 2\nu)C}{6F} \right] (1 - L_n) + 0.5(1 - K_0)(1 + J_n - 2N_n) \cos 2\theta \right\} \tag{3}$$

$$T = \frac{Pr^2}{2} \left\{ (1 + K_0)(1 - L_n) + (1 - K_0)(1 + J_n) \cos 2\theta \right\} \tag{4}$$

where  $K_0$  is the earth pressure coefficient at rest,  $\theta$  is the angle measured in counter-clockwise from horizontal plane,  $F$  is the flexibility

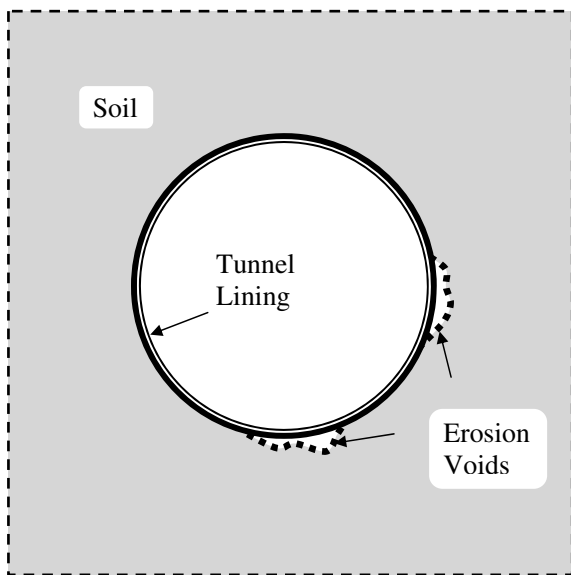


Fig. 1. Existing lining experiencing local support loss as a result of erosion voids.

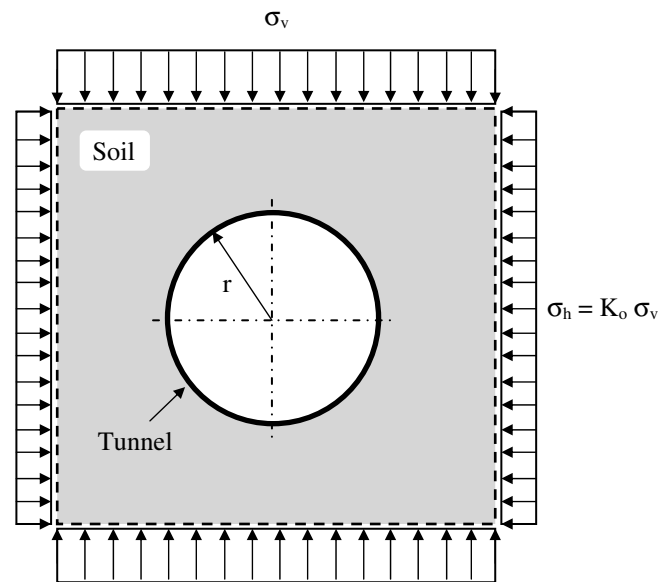


Fig. 2. Soil and liner under a state of in situ stress condition.

ratio and  $C$  is the compressibility ratio. The parameters  $L_n, J_n,$  and  $N_n$  used in Eqs. (1)–(3) are defined below

$$L_n = \frac{(1 - 2\nu)(C - 1)}{1 + (1 - 2\nu)C} \tag{5}$$

$$J_n = \frac{[(1 - 2\nu)(1 - C)]F - 0.5(1 - 2\nu)^2C + 2}{[(3 - 2\nu) + (1 - 2\nu)C]F + 0.5(5 - 6\nu)(1 - 2\nu)C + (6 - 8\nu)} \tag{6}$$

$$N_n = \frac{[1 + (1 - 2\nu)C]F - 0.5(1 - 2\nu)C - 2}{[(3 - 2\nu) + (1 - 2\nu)C]F + 0.5(5 - 6\nu)(1 - 2\nu)C + (6 - 8\nu)} \tag{7}$$

It should be noted that many of the analytical solutions are based on simplifying assumptions regarding the soil and the lining. The circular tunnel is usually assumed to be so deep that the increase of stress due to gravity can be ignored. Hence the soil is subjected to a uniform stress field. The lining is either rough (full bonding between the soil and the lining) or smooth (no bonding). Both lining and ground behave linearly elastic.

Bobet (2001) presented analytical solutions for a shallow tunnel in saturated ground considering two different drainage conditions, namely, full drainage at the ground-liner interface, and no drainage. The solutions covered different construction processes and soil conditions including (1) dry ground; (2) saturated ground with and without air pressure; (3) with and without a gap between the ground and the liner. The lining thrust,  $T,$  and bending moment,  $M,$  for the case of saturated ground condition is expressed by

$$T = \frac{1}{2} \frac{[2E_r w - \gamma h(1 + K_o)(1 + \nu)](C + F)}{(C + F)(1 + \nu) + (1 - \nu^2)CF} r - \frac{3}{2} \frac{\gamma h(1 - K_o)r \cos 2\theta}{(1 - \nu)F + 6} + \frac{\gamma(1 - K_o)r^2 \sin 3\theta}{(1 - \nu)F + 24} \tag{8}$$

$$M = -\frac{3}{2} \frac{\gamma h(1 - K_o)r^2 \cos 2\theta}{(1 - \nu)F + 6} + \frac{\gamma(1 - K_o)r^3 \sin 3\theta}{(1 - \nu)F + 24} \tag{9}$$

where,  $w$  is the gap between the shield and the liner;  $C$  and  $F$  are the compressibility and flexibility ratios;  $r$  is the tunnel radius;  $\theta$  is the angle measured in counter-clockwise from the springline. It has been concluded that the geometry of the tunnel, soil properties, and construction method affect the stresses in the liner and the settlements of the ground. It was also found that a smaller gap or a deeper tunnel produce larger stresses, while a stiffer ground or a smaller tunnel produce smaller stresses. It should be noted that the applicability of the analytical solutions as described by Bobet (2001) is limited to tunnels in homogeneous, isotropic soils, where the ground does not have extensive yielding.

As indicated earlier, ground pressure on linings depend heavily on the construction procedures (physical gap, lining installation method, workmanship, etc.). To incorporate the installation procedure, Chou and Bobet (2002) developed an analytical solution that accounts for the installation method using a displacement approach. They considered 28 shield tunnels to find values for the gap between lining and ground ranging from 10 mm to 128 mm, depending on tunnel radius. In this study, the theoretical values of the moment and thrust at the tunnel crown and springline are used to validate the finite element model before proceeding with the reported numerical investigation as detailed in the following section.

### 3. Numerical analysis

Finite element analyses are conducted to investigate the response of an existing liner installed in soft ground and experiencing a local loss of contact due to the presence of erosion voids. The tunnel is assumed to have a circular shape with a diameter of 4 m and to be constructed at a depth of 10 m below the ground surface

as shown in Fig. 3. Considering the symmetric condition of the tunnel, only one half of the tunnel is analyzed. The analyses are performed using Plaxis V8 software (Brinkgreve and Vermeer, 1998). A plain strain finite element model is used to represent the soil and the tunnel lining. The lining is modeled using 3-noded beam elements, whereas the soil is modeled using 9-noded triangular elements. A typical finite element mesh is shown in Fig. 4. The model is restrained in the horizontal direction at the symmetry axis (smooth rigid) and is restrained in both the vertical and horizontal directions at the lower boundary (rough rigid). Fully drained condition is assumed. The interaction between the lining and the soil is modeled using interface elements which allows for the interface condition to be simulated. A strength factor  $R_{int}$  is introduced to define the strength parameters of the interface relative to those of the original material.

A series of simplified circular voids were introduced at the invert and springline. The size of the voids was selected such that unsupported length of the lining ( $L_v$ ) increase in five increments representing 0%, 3% (actually 3.3), 7% (actually 6.7), 10% (actually 10.6), and 15% (actually 14.5) of the tunnel circumference. Fig. 5 shows a schematic of the simplified void geometry at the springline. It should be noted that the actual erosion voids are usually three-dimensional in shape; however, in this study the length of the void is assumed to be long enough in the direction of the tunnel

axis to facilitate the application of the two-dimensional finite element analysis.

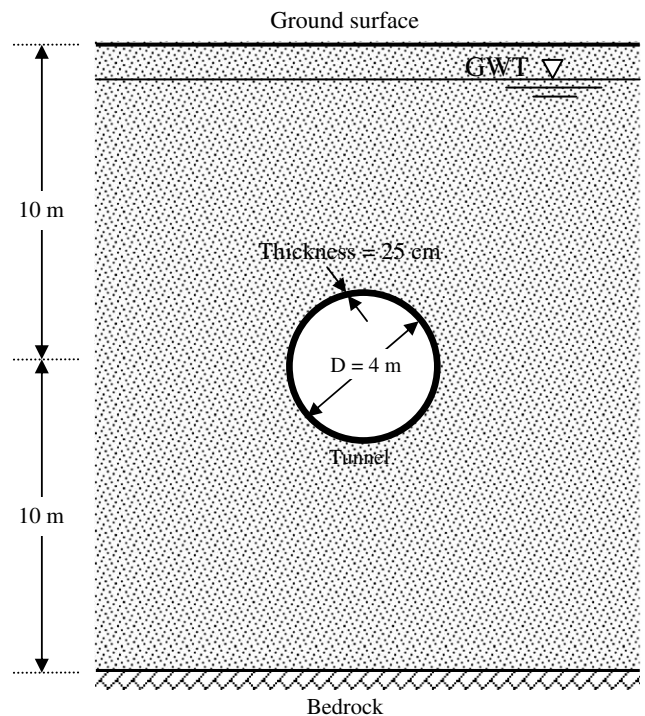


Fig. 3. Problem geometry used in the numerical analysis.

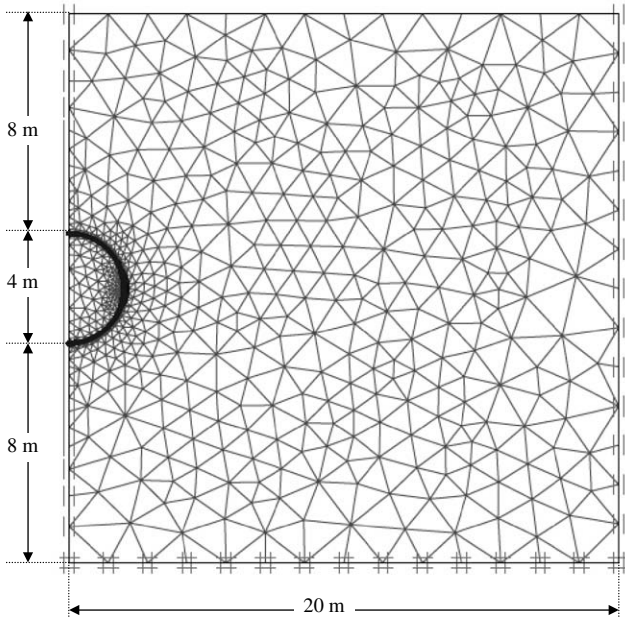


Fig. 4. Finite element mesh used in the numerical analysis. Note: mesh refined around the springline.

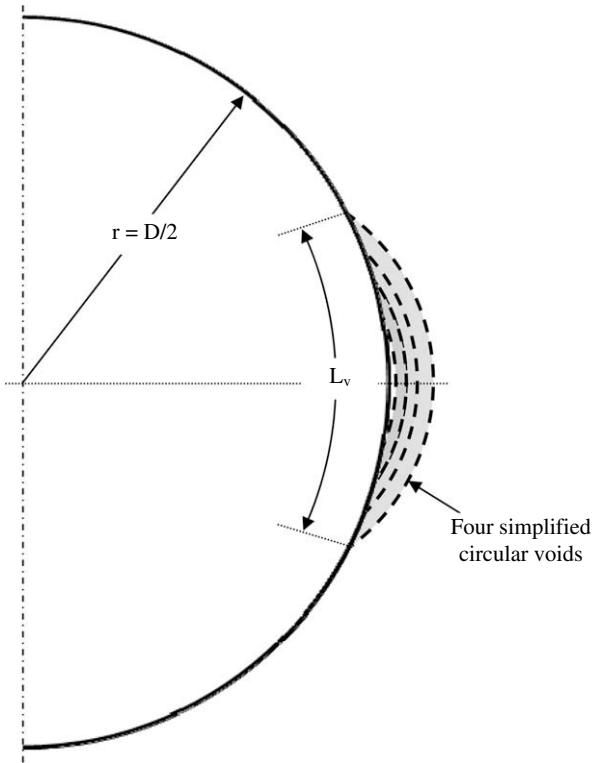


Fig. 5. Schematic of the simplified geometry of erosion voids located at the springline.

### 3.1. Modeling details

For the saturated sand material, the Hardening-Soil model (Schanz, 1998) as implemented in the Finite-Element code Plaxis (Brinkgreve and Vermeer, 1998) is used. A detailed description of this model is given in the program manual. Emphasis will be placed here on the meaning of the input parameters rather than describing the mathematical formulation of the model.

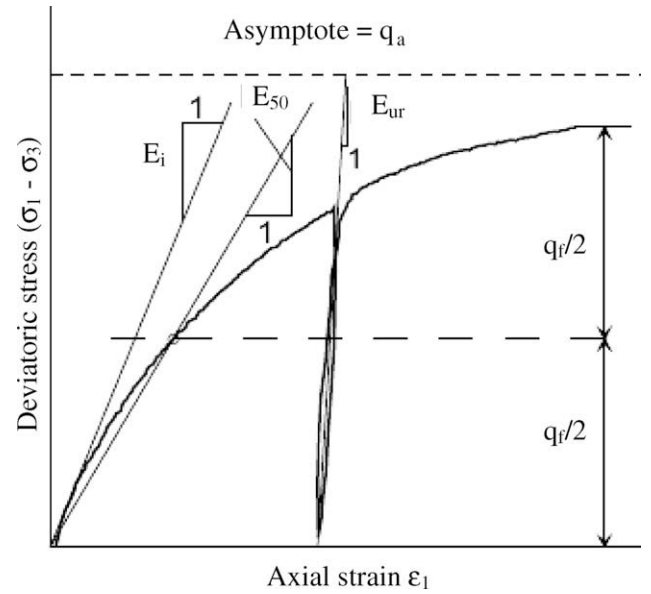


Fig. 6. Hyperbolic stress–strain relationship in primary loading for a standard drained triaxial test (Adapted from Plaxis User’s Manual, 2004).

*Soil stiffness parameters:* Fig. 6 shows a typical drained triaxial test with constant lateral pressure,  $\sigma_3$ . Under primary loading the behaviour is distinctly nonlinear and is assumed to be hyperbolic up to a failure stress. Here compressive stresses and strains are considered positive. While the maximum stress is determined by the Mohr–Coulomb failure criterion, the hyperbolic part of the curve is defined by using a single secant modulus as additional input parameter,  $E_{50}$ , as shown in Fig. 6. It determines the magnitude of both the elastic and the plastic strains. In contrast,  $E_{ur}$  is an elastic modulus. In conjunction with a Poisson’s ratio  $\nu_{ur}$ , the elastic modulus  $E_{ur}$  determines the soil behaviour under unloading and reloading; the indices ur stand for “unloading/reloading”. Both the secant virgin loading modulus  $E_{50}$  and the unloading modulus  $E_{ur}$  are stress-level dependent defined by

$$E_{50} = E_{50}^{ref} \left( \frac{ccot \phi - \sigma'_3}{ccot \phi + p^{ref}} \right)^m \quad (10)$$

$$E_{ur} = E_{ur}^{ref} \left( \frac{ccot \phi - \sigma'_3}{ccot \phi + p^{ref}} \right)^m \quad (11)$$

$E_{50}^{ref}$  and  $E_{ur}^{ref}$  are input parameters for a particular reference pressure  $p^{ref}$ . The exponent  $m$  can be measured both in oedometer tests and in triaxial tests and ranges between 0.4 and 1.0. A value of 0.5 is typical for sands whereas clays tend to have  $m \approx 1.0$ . The virgin oedometer stiffness,  $E_{oed}$ , for one-dimensional compression obeys a stress dependency according to the formula

$$E_{oed} = E_{oed}^{ref} \left( \frac{ccot \phi - \sigma'_1}{ccot \phi + p^{ref}} \right)^m \quad (12)$$

where  $E_{oed}^{ref}$  is a tangent stiffness at a vertical stress of  $-\sigma'_1 = p^{ref}$ .

In the special case of  $m = 1$  one obtains a linear stress-dependency as usual for cohesive material. In addition to  $E_{50}^{ref}$  and  $E_{ur}^{ref}$ , the oedometer modulus  $E_{oed}^{ref}$  is also an input parameter. Together with the parameters  $m$ ,  $\nu_{ur}$ ,  $\hat{c}$ ,  $\psi$  and the dilatancy angle,  $\psi$ , there are a total of eight material parameters. Often, no triaxial test results are available for determining  $\nu_{ur}$ ,  $E_{50}^{ref}$  and  $E_{ur}^{ref}$ , in which case one has to rely on oedometer results and general empirical data, such as  $\nu_{ur} = 0.1–0.2$ . For sands and stiff clays, one can mostly use  $E_{50}^{ref} = E_{ur}^{ref}$ . The elasticity modulus  $E_{ur}^{ref}$  can be determined directly from a triaxial test or indirectly with the help of oedometer results. If the unloading modulus from the oedometer test is termed  $E_{oed}^{ur}$ ,

according to isotropic linear elasticity the following relationship holds (Vermeer et al., 2002)

$$E_{ur} = (1 - 2\nu_{ur}) \frac{1 + \nu_{ur}}{1 - \nu_{ur}} E_{oed}^{ur} \quad (13)$$

Hence the proper estimates of  $E_{ur}$  can be calculated from  $E_{oed}^{ur}$ .

The stiffness properties of the saturated sand in this study are assumed based on the range of values proposed by Kempfert and Gebreselassie (2006) for  $\sigma_3/p^{ref}$  of about 1.0 as shown in Fig. 7. The assigned soil properties are listed in Table 1. These parameters were kept constant throughout the finite element simulations.

**Lining properties:** Tunnel lining is modeled using 3-noded beam elements with three degrees of freedom per node. The equivalent lining thickness is expressed as  $d_{eq} = \sqrt{12EI/EA}$  based on the flexural rigidity (bending stiffness),  $EI$ , and the axial stiffness,  $EA$ , of the lining cross section. To understand the role of flexibility ratio on the lining response to erosion voids, four different flexibility ratios were examined, namely, 16, 32, 64, and 128. Initial stress distribution in the tunnel lining was calculated considering a volume loss of 1% which represents an acceptable value for shield tunnelling in stable ground conditions (Attewell and Farmer, 1974; O'Reilly and New, 1982). Finite element model is first validated by comparing initial stresses in the lining (before voids are introduced) with analytical solutions as described in the following section.

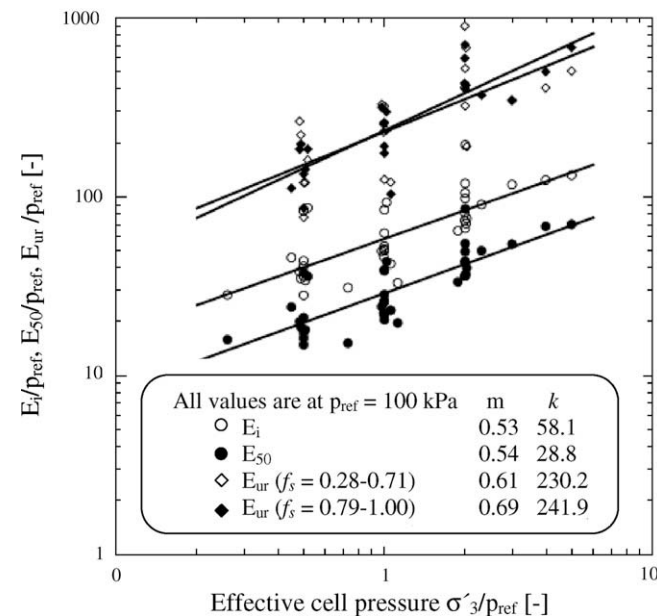


Fig. 7. The variation of the modulus of elasticity with confining pressure under CID test condition (Adapted from Kempfert and Gebreselassie, 2006).

Table 1  
Soil parameters for the hardening soil model

$E_{50}^{ref}$	$3 \times 10^4 \text{ kN/m}^2$
$E_{oed}^{ref}$	$2.5 \times 10^4 \text{ kN/m}^2$
$E_{ur}^{ref}$	$1.5 \times 10^5 \text{ kN/m}^2$
$\nu_{ur}$	0.20
$p^{ref}$	100 kN/m <sup>2</sup>
$\phi'$	30°
$M$	0.5
$\gamma_{sat}$	18 kN/m <sup>3</sup>
$\gamma_d$	16 kN/m <sup>3</sup>
$K_o$	0.5 and 1.0
$c^{ref}$	2 kN/m <sup>2</sup>

Table 2  
Lining and soil properties used in the model validation

<b>Lining properties</b>	
Lining radius	2 m
Thickness	0.25 m
EA	$8 \times 10^6 \text{ kN/m}$
EI	$8 \times 10^4 \text{ kN.m}^2/\text{m}$
<b>Soil properties</b>	
E	$1.5 \times 10^5 \text{ kN/m}^2$
$K_o$	0.426
$\nu$	0.3
$\gamma_d$	16 kN/m <sup>3</sup>

Table 3  
Comparison between the numerical and closed form solutions

Method	Moment (kN m/m)		Thrust (kN/m)	
	Springline	Invert	Springline	Invert
Numerical	-44.5	57.6	848.4	9768.3
Bobet (2001)	-47.9	54.7	876.4	9223.1

### 3.2. Validation of the numerical model

Elastic analysis has been conducted to validate the numerical model using the same tunnel geometry and finite element mesh described earlier in Figs. 3 and 4. The calculated initial stresses in the lining have been compared with the closed form solutions of Bobet (2001). The properties of the soil and tunnel lining used in the analysis are given in Table 2.

The calculated bending moments and thrust forces at the tunnel crown and springline are summarized in Table 3. The negative sign of the moment at the springline indicates that the outer fiber of the lining is subjected to tensile bending stress. It can be seen that the numerical solution predicted a slightly higher moment and thrust values at the crown with a maximum difference of about 5% whereas a slightly lower values were calculated at the springline. This indicated a general agreement between the numerical and analytical solutions.

## 4. Results and discussion

The effect of erosion voids on the circumferential stresses in the lining is investigated by examining the changes in bending moments and thrust forces as the void is introduced and incrementally increased in size at the tunnel invert and springline. The void size is expressed using the ratio ( $L_v/\pi D$ ) that relates the unsupported length,  $L_v$ , and the lining circumference,  $\pi D$ , in all presented figures. It should be mentioned that soil stresses generally increased in the close vicinity of the void as the void size increased. For voids introduced at the springline, the stresses were found to exceed the soil shear strength (causing soil failure) when the unsupported length of the tunnel,  $L_v$ , reached about 10.6% of the lining circumference. This is indicated by the arrows shown on the relevant figures (Figs. 8, 9, 12 and 13).

### 4.1. Effect of void size on bending moment

The calculated bending moments at the springline and invert are presented in Figs. 8–11 for the two cases of  $K_o = 0.5$  and  $K_o = 1$ , respectively. The presented values are normalized by dividing the calculated moments,  $M$  (kN m/m), by  $\gamma z r^2$ , where,  $\gamma$  (kN/m<sup>3</sup>) is the saturated unit weight of the soil,  $z$  (m) is the depth to the tunnel centerline, and  $r$  (m) is the tunnel radius. Peck et al. (1972) reported that for a flexibility ratio,  $F$ , of more than 10, the lining system is considered to be flexible. In this study, four

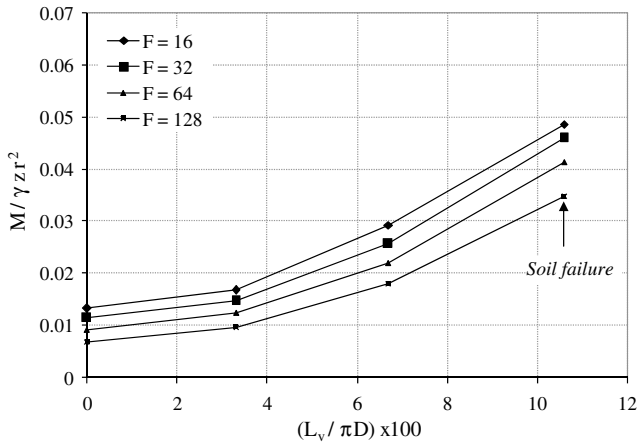


Fig. 8. Bending moment at the tunnel springline as a function of the void size: ( $K_o = 0.5$ ).

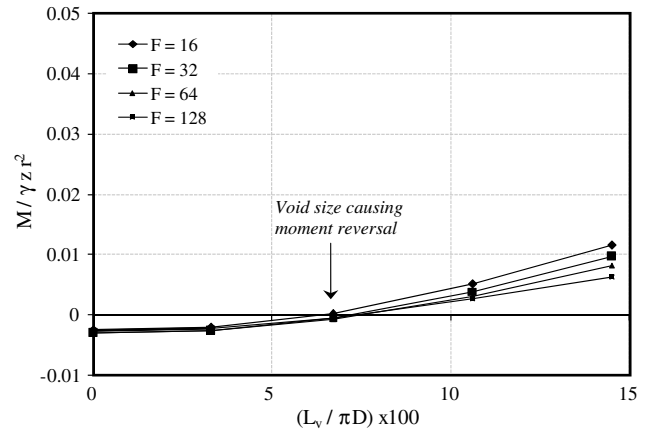


Fig. 11. Bending moment at the tunnel invert as a function of the void size: ( $K_o = 1$ ).

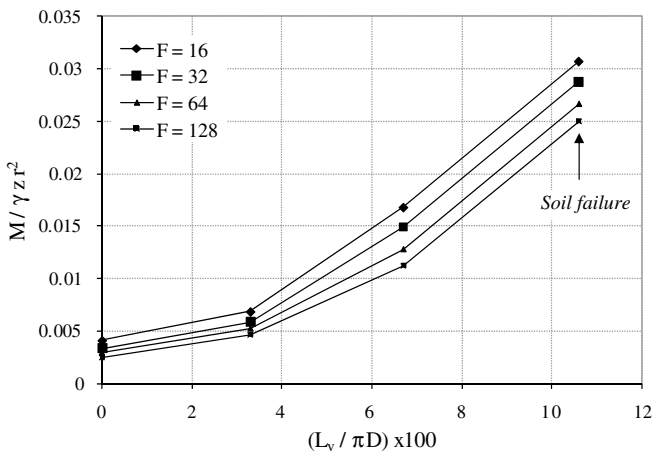


Fig. 9. Bending moment at the tunnel springline as a function of the void size: ( $K_o = 1$ ).

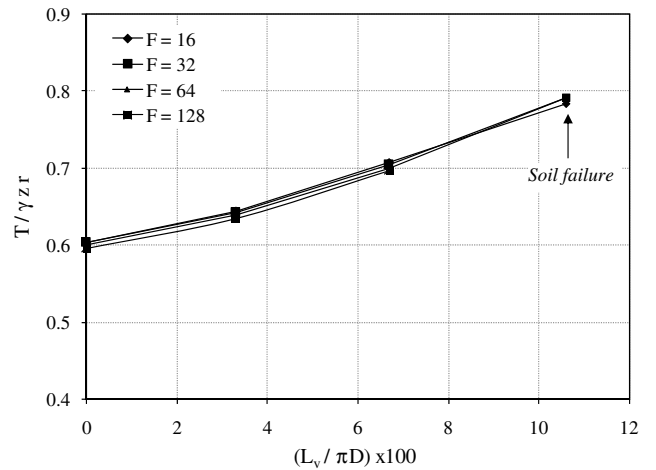


Fig. 12. Thrust at the tunnel springline as a function of the void size: ( $K_o = 0.5$ ).

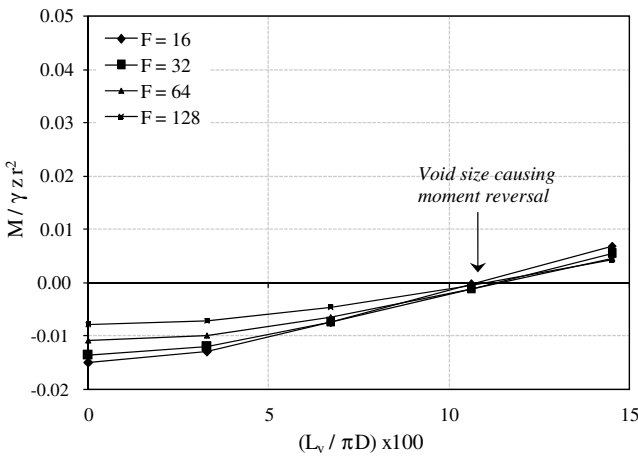


Fig. 10. Bending moment at the tunnel invert as a function of the void size: ( $K_o = 0.5$ ).

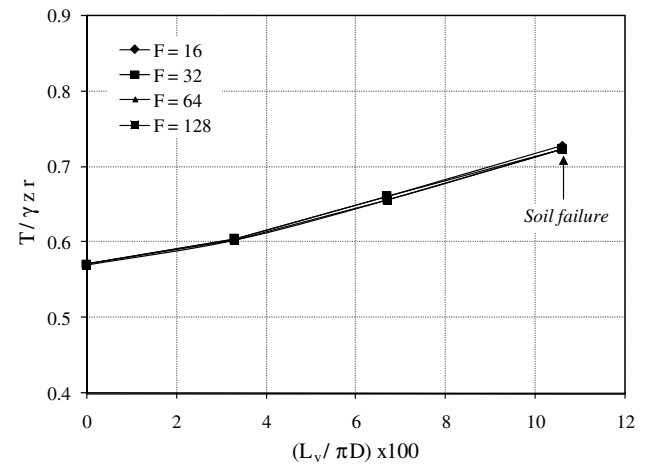


Fig. 13. Thrust at the tunnel springline as a function of the void size: ( $K_o = 1$ ).

different flexibility ratios were chosen, namely,  $F = 16, 32, 64$  and  $128$  which represent relatively flexible lining systems.

At the springline: Figs. 8 and 9 show the relationships between the normalized void sizes  $(L_v/\pi D)$  and bending moment ratios at

the tunnel springline. The moment ratio generally increased as  $F$  decreased from  $128$  to  $16$ . For a given flexibility ratio, significant increase in bending moment was calculated when the void size increased from  $3.3\%$  to  $10.6\%$  of the tunnel circumference. By examining Figs. 8 and 9, it can be seen that the moment changes accelerate once the void size reaches about  $3\%$ . It was also observed

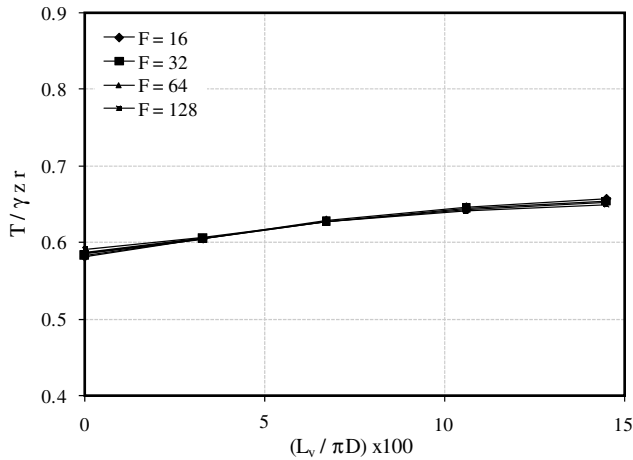


Fig. 14. Thrust at the tunnel invert as a function of the void size: ( $K_0 = 0.5$ ).

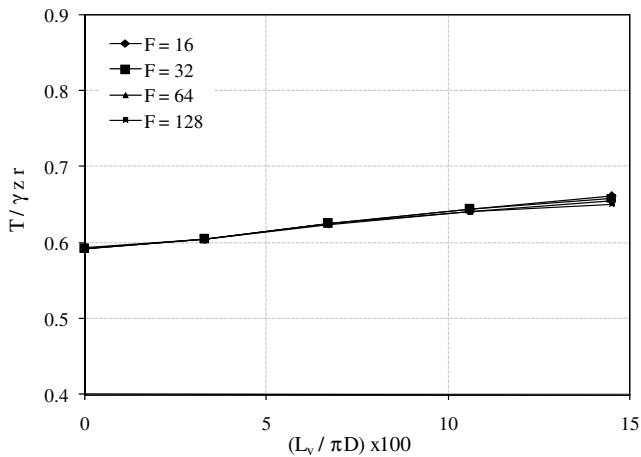


Fig. 15. Thrust at the tunnel invert as a function of the void size: ( $K_0 = 1$ ).

that the calculated bending moments for  $K_0 = 1$ , were generally smaller as compared to the case of  $K_0 = 0.5$ .

At the invert: Figs. 10 and 11 present the changes in bending moments at the invert for  $K_0 = 0.5$  and 1, respectively. Bending moments decreased slowly as the void size increased and the sign reversed from negative to positive as the void size (represented by  $L_v$ ) reached about 11% of the tunnel circumference for  $K_0 = 0.5$  and about 7% for  $K_0 = 1$ . The above finding implies that the inner fibers of the tunnel lining (that were initially in compression) will be subjected to tensile stresses if erosion voids are to develop at the invert and grow in size to exceed certain threshold. By inspecting Figs. 10 and 11, it can be seen that the threshold of void size that causes moment reversal is almost independent of the flexibility ratio for the investigated range of soil properties and in-situ stress conditions.

4.2. Effect of void size on lining thrust

Figs. 12–15 present the relationship between the lining thrust and normalized void size for different flexibility ratios and  $K_0$  conditions. The calculated thrusts,  $T$  (kN/m), were normalized with respect to the saturated unit weight of the soil,  $\gamma$  (kN/m<sup>3</sup>), the depth to the tunnel centerline,  $z$  (m), and the tunnel radius,  $r$  (m).

At the springline: Figs. 12 and 13 show the relationship between the normalized void sizes and the maximum thrust ratios at the tunnel springline. Very similar trends were observed for the cases of  $K_0 = 0.5$  and 1. Thrust ratios were found to increase slowly up to a normalized void size of about 3% of the tunnel circumference. This was followed by a rapid increase as the void grew further in size. Flexibility ratio was found to have insignificant effects on the changes in thrust ratios at the springline.

At the invert: Changes in thrust ratios were found to increase initially with a slow rate up to a normalized void size of about 10% of the tunnel circumference as shown in Figs. 14 and 15 for  $K_0 = 0.5$  and 1, respectively. Further increase in void size did not correspond to significant changes in the magnitude of the calculated thrust. Same trend was observed for the two cases of  $K_0 = 0.5$  and 1.0. In addition, the increase in flexibility ratio from 16 to 128 did not have any effects on the magnitude or the rate of change in the thrust ratios.

To visualize the relative changes in thrust and moment along the tunnel circumference, the above results are summarized in Figs. 16 and 17 for a given flexibility ratio ( $F = 16$ ). For  $K_0 = 0.5$ , thrust increased by 7%, 18% and 33 % which corresponded to void sizes of 3.3%, 6.7% and 10.6%, respectively, as shown in Fig. 16. The moment, on the other hand, increased by 27%, 120% and

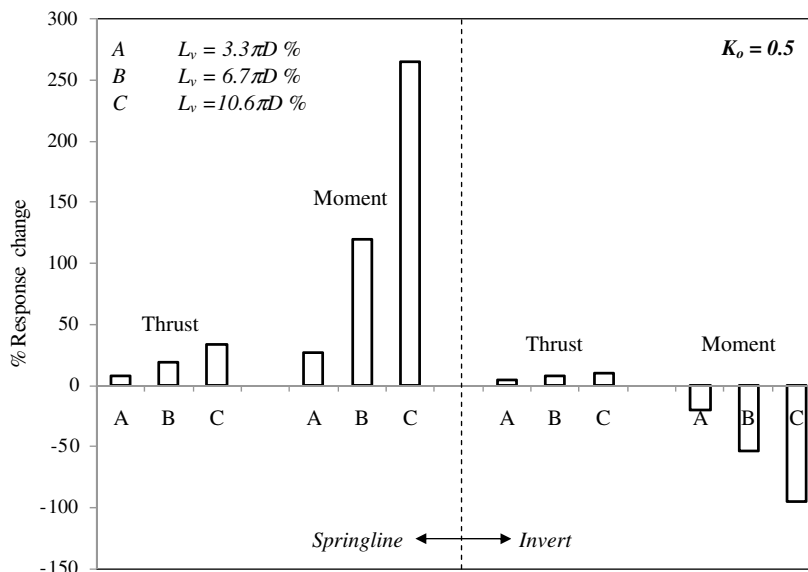


Fig. 16. Percentage change in lining response due to the introduction of voids for  $F = 16$  ( $K_0 = 0.5$ ).

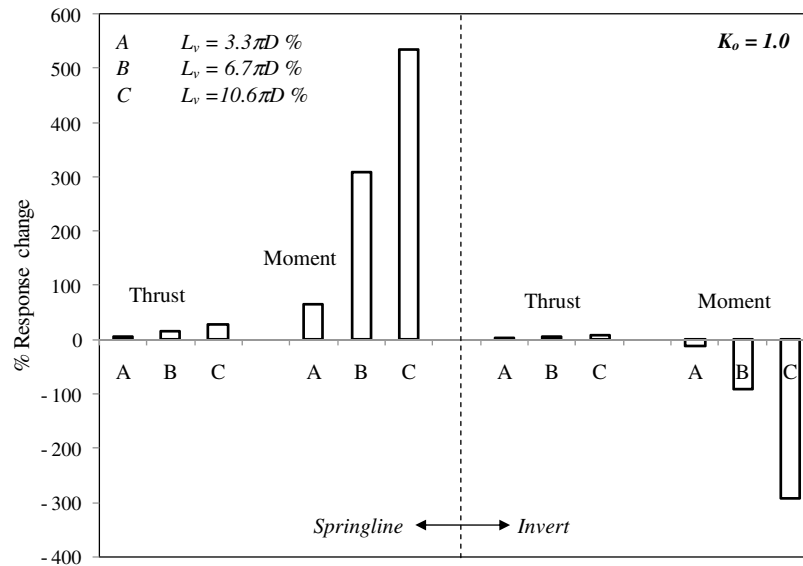


Fig. 17. Percentage change in lining response due to the introduction of voids for  $F=16$  ( $K_0=1.0$ ).

265% in excess of the design values. This is considered to be significant changes that could lead to undesirable stress levels in the tunnel lining. By examining the changes at the invert, the thrust increased by 4%, 7% and 10% and the moment decreased by 20%, 53% and 95%. Although the changes at the invert were relatively smaller compared to the springline, the reversal in the moment sign could render the effects to become significant. As  $K_0$  increased from 0.5 to 1.0, the changes almost doubled as shown in Fig. 17.

The investigation indicates that the increase of the normalized moment ratio was more evident for void size and implies that if a void becomes relatively large with respect to the tunnel circumference, the induced change in bending moment in the lining is affected by the location of the void and in situ stress conditions.

## 5. Summary and conclusions

The structural behaviour of a tunnel liner was investigated numerically with the controlled parameters including flexibility ratio, coefficient of earth pressure at rest, and void size, and the following conclusions are drawn from the results with the conditions and assumptions given in this study.

- (1) The investigations indicated that the response of an existing tunnel liner is affected by the presence of erosion voids around the tunnel circumference.
- (2) The increase of the normalized moment and thrust ratios was found to be dependent on the void size and the earth pressure coefficient at rest, and the larger the void size and earth pressure coefficient, the bigger the increase of the normalized moment and thrust ratios at the tunnel springline.
- (3) The effects were found to be more critical at the tunnel invert. The moment reversed its sign from negative to positive indicating possible cracking in the liner if the tensile strength of the lining material is to be exceeded.
- (4) Efforts should be made to detect and arrest erosion voids before excessive increase in lining stresses develop leading to costly failure.

It should be noted that the above conclusions are based on simplified 2D analysis of a problem that may involve 3D void geometry of irregular shape, size and location. In addition, the reported results are applicable to cases where the examined tunnels are con-

structed in soft ground represented by the Mohr-Coulomb material model. All results presented are theoretical in nature, and physical testing is needed to evaluate the performance of these calculations.

## Acknowledgement

This research is supported by the Fonds Québécois de la Recherche sur la Nature et les Technologies (FQRNT) and the Natural Sciences and Engineering Research Council of Canada (NSERC).

## References

- Attewell, P.B., Farmer, I.W., 1974. Ground deformations resulting from tunnelling in London clay. *Canadian Geotechnical Journal* 11 (3), 380–395.
- Attwell, P.B., 1978. Ground movements caused by tunnelling in soil. In: *Proceedings of Large Ground Movements and Structures Conference*. Cardiff. Pentish Press, London, pp. 812–948.
- Augarde, C.E., Burd, H.J., 2001. Three-dimensional finite element analysis of lined tunnels. *International Journal for Numerical and Analytical Methods in Geomechanics* 25, 243–262.
- Bobet, A., 2001. Analytical solutions for shallow tunnels in saturated ground. *Journal of Engineering Mechanics-ASCE* 127 (12), 1258–1266.
- Brinkgreve, R.B.J., Vermeer, P.A., 1998. PLAXIS-version 7. Finite-element code for soil and rock analyses User's Manual. A.A. Balkema, Rotterdam, The Netherlands.
- Bull, A., 1944. Stresses in the linings of shield driven tunnels. *Journal of Soil Mechanics and Foundation Division ASCE*, 1363–1394.
- Chen, W., Baldauf, S., 1994. Prediction of ground deformations due to excavation - Application to tunnel lining design in weak rock. In: *Proceedings of the 8th International Conference on Analytical and Computational Methods in Geomechanics*, West Virginia, USA, vol. 3, pp. 2565–2570.
- Chou, W., Bobet, A., 2002. Predictions of Ground Deformations in Shallow Tunnels in Clay. *Tunnelling and Underground Space Technology* 17, 3–19.
- Einstein, H.H., Schwartz, C.W., 1979. Simplified analysis for tunnel supports. *Journal of the Geotechnical Engineering Division, American Society of Civil Engineers* 105, 499–518.
- Engelbreth, K., 1961. Correspondence on Morgan, H.D., A contribution to the analysis of stress in a circular tunnel. *Geotechnique* 11 (3), 246–248.
- Kempfert, G., Gebreselassie, B., 2006. *Excavations and Foundations in Soft Soils*. Springer Berlin Heidelberg, New York, pp. 57–116.
- Kolymbas, D., Wagner, P., 2007. Groundwater ingress to tunnels-The exact analytical solution. *Tunnelling and Underground Space Technology* 22, 23–27.
- Leca, E., Clough, W., 1992. Preliminary design for NATM tunnel support in soil. *Journal of Geotechnical Engineering* 118 (4), 558–575.
- Lee, K.M., Rowe, R.K., 1990. Finite element modeling of the three-dimensional ground movements due to tunnelling in soft cohesive soils: Part 2-Results. *Computers and Geotechnics* 10, 111–138.
- Loganathan, N., Poulos, H.G., 1998. Analytical prediction for tunnelling-induced ground movements in clays. *Journal of Geotechnical and Geoenvironmental Engineering-ASCE* 124 (9), 846–856.

- Mair, R.J., Gunn, M.J., O'Reilly, M.P., 1981. Ground movements around shallow tunnels in soft clay. In: *Proceedings of the Tenth ICSMFE, Stockholm*, pp. 323–328.
- Mair, R.J., Taylor, R.N., Bracegirdle, A., 1993. Subsurface settlement profiles above tunnels in clays. *Geotechnique* 43 (2), 315–320.
- Morgan, D.H., 1971. A contribution to the analysis of stress in a circular tunnel. *Geotechnique* 11 (3), 37–46.
- Muir Wood, A.M., 1975. The circular tunnel in elastic ground. *Geotechnique* 1, 115–127.
- O'Reilly, M.P., New, B.M., 1982. Settlements above tunnels in the UK—Their magnitude and prediction. In: *Proceedings of Tunnelling'82, IMM, London*, pp. 173–181.
- Peck, R.B., 1969. Deep excavations and tunneling in soft ground. In: *Proceedings of the seventh International Conference on Soil Mechanics and Foundation Engineering, Mexico City*, pp. 225–290.
- Peck, R.B., Hendron, A.J., Mohraz, B., 1972. State of the art of soft-ground tunneling. In: *Proceedings of the North American Rapid Excavation and Tunneling Conference, Chicago, IL*, pp. 259–286.
- Sagaseta, C., 1987. Analysis of undrained soil deformation due to ground loss. *Geotechnique* 37 (3), 301–320.
- Schanz, T., 1998. On the modelling of mechanical behaviour of frictional materials (Zur Modellierung des Mechanischen Verhaltens Von Reibungsmaterialien). Habilitation Dissertation, University of Stuttgart (in German).
- Schmid, H., 1926. *Statische Probleme des Tunnel-und Druckstollenbaues*, Berlin 1926.
- Schmidt, B., 1974. Prediction of settlements due to tunneling in soil: three case histories. In: *Proceedings of the second Rapid Excavation and Tunneling Conference, San Francisco*, vol. 2, pp. 1179–1199.
- Schulze, H., Duddeck, H., 1964. Stresses in shield driven tunnels. *Beton and Stahlbetonbau* 8, 169–175.
- Swoboda, G., Mertz, W., Schmid, A., 1989. Three dimensional numerical models to simulate tunnel excavation. In: *Proceedings of NUMLOG III. Elsevier Science Publishers Ltd., London*, pp. 536–548.
- Talesnick, M., Baker, R., 1999. Investigation of the failure of a concrete-lined steel pipe. *Geotechnical and Geological Engineering* 17, 99–121.
- U.S. Department of Transportation, 2005. *Federal Highway Administration. Highway and Rail Transit Maintenance and Rehabilitation Manual*, pp. 4-1–4-36. (Chapter 4).
- Vermeer, P.A., Marcher, T., Ruse, N., 2002. On the Ground Response Curve. *Felsbau. Rock and Soil Engineering* 20 (6), 19–24.
- Verruijt, A., Booker, J.R., 1996. Surface settlements due to deformation of a tunnel in an elastic half plane. *Geotechnique* 46 (4), 753–756.